

Research Paper

Enriched Brain Omega-3 Polyunsaturated Fatty Acids Confer Neuroprotection against Microinfarction

Chuanming Luo^{a,b,1}, Huixia Ren^{a,1}, Xiaoli Yao^c, Zhe Shi^a, Fengyin Liang^c, Jing X. Kang^d, Jian-bo Wan^a, Zhong Pei^c, Kuan-Pin Su^e, Huanxing Su^{a,*}

^a State Key Laboratory of Quality Research in Chinese Medicine, Institute of Chinese Medical Sciences, University of Macau, Macao, China

^b Department of Neurology, Seventh Affiliated Hospital, Sun Yat-Sen University, Shenzhen 510080, China

^c Department of Neurology, National Key Clinical Department and Key Discipline of Neurology, First Affiliated Hospital Sun Yat-Sen University, Guangzhou 510080, China

^d Laboratory for Lipid Medicine and Technology, Department of Medicine, Massachusetts General Hospital, Harvard Medical School, Boston, MA, USA

^e Department of Psychiatry & Mind-Body Interface Laboratory (MBI-Lab), China Medical University Hospital, College of Medicine, China Medical University, Taichung, Taiwan



ARTICLE INFO

Article history:

Received 17 February 2018

Received in revised form 10 May 2018

Accepted 23 May 2018

Available online 5 June 2018

Keywords:

Fish oil

Cognitive decline

Vascular dementia

Neuropsychiatric disorders

ABSTRACT

Cerebral microinfarcts have significant effects on the development of geriatric neurological disorders, including vascular dementia and Alzheimer's disease. However, little is known about the pathophysiological mechanisms involved in the evolution of microinfarcts and potential treatment and prevention against these microvascular ischemic lesions. In the present study, the "single cortical microinfarct model" generated via occluding a penetrating arteriole by femtosecond laser ablation and the "multiple diffuse microinfarcts model" induced by unilateral injection of cholesterol crystals through the internal carotid artery were established to investigate the pathophysiological mechanisms underlying the evolution of microinfarcts and the effects of omega-3 polyunsaturated fatty acids (ω -3 PUFAs) on alleviating microinfarct burdens and functional deficits. The occlusion of a single penetrating arteriole led to a distinct cortical microinfarct, which manifested as neuronal loss and occupation of activated glial cells in the ischemic core. Using *Fat-1* transgenic mice and fish oil supplements, we demonstrated that both endogenously-generated and exogenously-delivered ω -3 PUFAs significantly inhibited the activation of receptor-interacting serine/threonine protein kinases 1 (RIPK1) and its downstream apoptosis-associated proteins, mitigated cell apoptosis, and anatomically reduced the microinfarct size. The protective effects of ω -3 PUFAs against microinfarcts were further verified in a multiple diffuse microinfarcts model, where ω -3 PUFAs significantly attenuated cell apoptosis as revealed by TUNEL staining, alleviated the diffuse microinfarct burdens and remarkably improved the functional deficits as evidenced by reduced spontaneous anxiety, increased preference for the novel object, and improved hippocampal-based learning and short-term memory. Together, these findings demonstrate that enriched brain ω -3 PUFAs are effective for reducing microinfarct burdens and improving the function deficits, which support the clinical research and application of ω -3 PUFAs in the treatment or prophylaxis in vascular dementia.

© 2018 The Authors. Published by Elsevier B.V. This is an open access article under the CC BY-NC-ND license (<http://creativecommons.org/licenses/by-nc-nd/4.0/>).

1. Introduction

Accumulating evidence suggests that cerebral microinfarcts have significant effects on the development of neuropsychiatric disorders [3,29]; Knopman, 2012; [10]. In post-mortem studies, cerebral microinfarcts are abundantly detected in the brain of patients with mild cognitive impairment (MCI) [14], vascular dementia (VaD) [9], Alzheimer's disease (AD) [33], and depression [1,45]. Furthermore, advanced neuroimaging technology provides compelling anatomical

evidence that cerebral microinfarcts are prevalent in aging people with various brain disorders, including VaD [27,32], MCI [15,44], depression [36], and AD [28,42].

Cerebral microinfarct is defined as microscopic vascular occlusion <1 mm (mm) in size, which results from a variety of cerebral small vessel diseases, such as vessel lumen occlusion, arteriosclerosis and vascular wall inflammation [3]. Although the definite pathogenesis of cerebral microinfarcts remains unknown, it has been proposed that neuroinflammation, oxidative stress and apoptosis might be the main triggering factors [42]. However, little is known about the pathophysiological mechanisms underlying the evolution of microinfarcts and the causal effects of microinfarcts on neuropsychiatric manifestation. With the growing health burden of dementia and depression in the aged population worldwide, it is urgently important now to understand the

* Corresponding author at: State Key Laboratory of Quality Research in Chinese Medicine, Institute of Chinese Medical Sciences, University of Macau, Macao, China.

E-mail address: huanxingsu@umac.mo (H. Su).

¹ These authors contributed equally to this work.

etiology, pathophysiological alterations and functional consequences of cerebral microinfarcts, as well as to develop effective and safe approaches for the treatment and prevention against the development of microinfarcts.

Omega-3 polyunsaturated fatty acids (ω -3 PUFAs) are highly enriched in the central nervous system and serve as an important structural component to maintain cellular functional integrity [35,41]. In the past decades, a series of epidemiological studies and clinical trials have suggested that increasing dietary intake or nutritional supplementation of ω -3 PUFAs, particularly long-chain PUFAs like docosahexaenoic acid (DHA) and eicosapentaenoic acid (EPA), is closely associated with a reduced risk to or therapeutic effects on cognitive disorders [2,12,49]. Moreover, increased intake of ω -3 PUFAs has been reported to significantly improve behavioral, neurological and histological outcomes in focal ischemic stroke models by modulating inflammatory, anti-oxidative, neurotrophic, and anti-apoptotic responses [4,6,13,30,39]. However, no previous study has investigated the effects of ω -3 PUFAs on microinfarcts. Accordingly, it is of great interests to determine whether ω -3 PUFAs can attenuate microinfarcts and improve cognitive impairments related to microinfarcts.

In the present study, we established a single microinfarct model by occlusion of a cortical penetrating arteriole with focused femtosecond laser pulses. In addition, the multiple diffuse microinfarcts model was implemented using unilateral injection of cholesterol crystals through the internal carotid artery. Our aims were to investigate the molecular and cellular responses to the formation of microinfarcts and evaluate the potential therapeutic effects of ω -3 PUFAs on alleviating microinfarcts and cognitive impairment.

2. Materials and Methods

2.1. Animals and Dietary Supplementation

All animal studies were conducted following prevailing laws and institutional guidelines on the humane care and use of laboratory animals and were approved by the ethical committee of the University of Macau and Sun Yat-Sen University. In all the experiments, 8–10-week old male *Fat1* transgenic mice and C57BL/6J mice (22–24 g) were used. Mice were housed in a temperature-controlled room at 25 °C with a 12:12 h light-dark cycle and ad libitum access to food and water. Male heterozygous *Fat1* mice were obtained from Dr. Jing X. Kang, Harvard Medical School (Cambridge, MA, USA) and used to mate with female C57BL/6 mice to generate heterozygous *Fat1* mice and wild type (WT) littermates for experimental studies. The transgenic mouse carries a *Fat1* gene that converts ω -6 PUFAs into ω -3 PUFAs, leading to the abundance of ω -3 PUFAs and a high ω -3 PUFAs / ω -6 PUFAs ratio in tissues [11]. A modified diet containing 10% corn oil (TROPIC Animal Feed High-tech Co., Ltd., China), with a fatty acid profile high in ω -6 PUFAs (mainly linoleic acid) and low in ω -3 PUFAs (~0.1% of the total fat supplied) was given. Accordingly, *Fat1* mice provided a suitable model to investigate the effects of endogenous ω -3 PUFAs.

The advance proper fish oil (containing 60% DHA and 15% EPA, Wuhan Sheng Tian Yu Biotechnology CO., LTD, China) was given to adult C57BL/6 mice (30 mg/kg weight) through daily oral gavage for 3 weeks prior to the subsequent experiments. Control animals received intragastric administration of equivoluminal isocaloric corn oil daily for 3 weeks prior to the subsequent experiments.

2.2. Fatty Acid Analysis

To evaluate the effects of the expression of the *Fat1* gene and the dietary regime on the PUFA composition in the brain cortex, the cortical tissue samples of mice from the experimental groups ($n = 3$ per group) were dissected and processed for fatty acid analysis by gas chromatography–mass spectrometry (GC–MS). Quantifications were performed by an investigator who was blind to the animal grouping and

carried out by normalizing individual peak areas as the percentage of total fatty acids.

2.3. Penetrating Arteriole Occlusion (PAO)

Mice were deeply anesthetized with 5% isoflurane, and then maintained at 2.5%, in oxygen with the anesthesia machine (RWD Life Science Co., Ltd., Shenzhen, China). To develop a model of penetrating arteriole occlusion (PAO) using two-photon microscopy, a thinned-skull window was prepared. Briefly, after the animal was placed in a stereotaxic apparatus, an incision with a sterile scalpel was made through the middle scalp skin of the mouse, and the skull bone was exposed by scraping away the periosteum. A 2×2 mm² region thinned-skull window was made over the left somatosensory cortex, which greatly minimizes disruption of the intracranial milieu. To image the vascular structure, the blood was labeled by intravenous injection of fluorescein isothiocyanate-dextran (FITC, 2000 kDa, FITC-d2000, 1.5% in saline, Sigma-Aldrich, Saint Louis, MO, USA) through the tail vein. To generate the PAO by damaging the endothelium of targeted vessels, intensively focused femtosecond laser pulses with a Ti:Sapphire laser (Coherent Chameleon Ultra II, CA) was used as a light source tuned at 800 nm with 140 fs pulse width and 80 MHz repetition rate [25,26,37]. The vascular injury was induced using the point bleach mode. The 6 points (one second per point) were focused on the two edges of the lumen of the target vessel in the same plane. To minimize possible collateral damage or avoid bleeding, the endothelium of the target vessel was damaged with an 800-nm laser, whose intensity (Max. power 3.5 W) was controlled by setting the electro-optic modulator (EOM) at 30% (roughly 1.05 W at the plane). In most cases, this injury triggered the natural clotting cascade, leading to localized clotting in the vessel. If the occlusion did not occur, we gradually increased the intensity by ~10% each time until the minimum power necessary to trigger clot formation in the target vessel was reached. The irradiation was repeated in case of recanalization (within 3 h after the injury). If vascular rupture occurred, the animal was excluded from the study. Overall, the incidence of vascular rupture is 4% (3 out of a total of 75 mice). Persistent occlusion was confirmed at 24 h by visual inspection and two-photon imaging. No death occurred in the PAO experiment.

2.4. In Vivo two-Photon Microscopy Imaging

To develop the model of PAO and evaluate the dynamic evolution of microcirculation and propidium iodide (PI)-staining after PAO, a Leica NA 0.95 and the 25 \times magnification water-immersion objectives were used. All images were acquired by using two-channel NDD detection with emission filter 525/50 nm and 585/40 nm under the same imaging parameters (laser power, photomultiplier tube voltage and gain) on a TCS SP5 MP System (Leica Microsystems, Mannheim, Germany). The person who performed image acquisition and image analysis was blind to the experiment.

2.5. The Volume of Blood Flux

The flux of the vessel of interest (F) was evaluated as described previously [37]. Briefly, the diameter of the penetrating arteriole of interest (d) was determined from at least 20 movie frames located in the surface segment of the penetrating arteriole. We used line scan to measure the centerline red blood cell (RBC) velocity (v) in individual vessels of interest at a line rate of 700 Hz. The centerline RBC velocity was automatically calculated with the Leica LAS AF 2.5 software. The average centerline RBC velocity for 30 s was referred to as the RBC speed of the vessels of interest. The flux of the vessel of interest (F) is equal to $\pi/8 v (0) d^2$. The measurement was performed by an investigator who was blind to the experiment.

2.6. Transcranial Propidium Iodide (PI)-Staining

To analyze the evolution of cell death after PAO, transcranial PI staining was used. PI is a sensitive marker for membrane integrity and able to identify irreversible cell damage [34,38]. An elegant recent study demonstrated that PI can easily pass through the intact murine thin-skull to label dead parenchymal cells [34]. Accordingly, we detected cell death in vivo by transcranial application of PI. Briefly, the experimental animal was fixed with a custom-built metal frame by holding the head with a cyanoacrylate glue and dental cement. Surgical incision was performed on the skull scalp and the skull bone was exposed after clearing the external periosteum with sterilized tampons. The skull bone was thinned to approximately 30 μm with a microdrill. The thinned-skull area was incubated with PI (1.5 mM) in artificial cerebrospinal fluid (aCSF) for 30 min, and then followed by a single wash with aCSF and immediately imaging by two-photon microscopy, using a Leica NA 0.95, 25 \times magnification water-immersion objective. Stacks of images were acquired using a step size of 2.0 μm to a depth of 250 μm . Dead cells from 0 to 50 μm below the thinned-skull were considered meningeal, while cells from 50 to 250 μm were considered parenchymal. The dead cells in the parenchyma were analyzed and the number of dead cells was represented as cells per mm^3 . Cells labeled by PI, with red fluorescence, were considered to be dead cells. The number of PI-positive cells in the 3-D stacks was counted as described previously [31] using the Leica LAS AF 2.5 software. The quantifications were performed by an investigator who was blind to the experiment.

2.7. Multiple Diffuse Microinfarcts Model

To develop the multiple diffuse microinfarct model, cholesterol crystals (Sigma-Aldrich, Saint Louis, MO, USA) were first filtered through a 70- μm sieve followed by a 40- μm cell strainer, and then resuspended in saline and counted with a hemocytometer. After the animal was anesthetized, we carefully exposed the right common carotid artery (CCA), internal carotid artery (ICA) and external carotid artery (ECA) under a dissecting microscope. The ICA was temporarily ligated, and the distal portion of the ECA was permanently ligated. Subsequently, we clipped the CCA and the proximal parts of the ECA and ICA, and made an incision between the ligation site and the clip site. Then, a polyethylene tube was inserted into the ECA, extending to the CCA. Around 3000 cholesterol crystals in 100 μl of saline or 100 μl saline alone (for sham animals) were injected through the tube after removal of the microvascular clip. The tube was eventually taken out, and the wound was closed after the proximal ECA was permanently ligated. A total of 12 mice out of 48 mice died after induction of multiple diffuse microinfarcts.

2.8. Physiological Monitoring

During the period of surgery and imaging, rectal temperature was maintained at 37 ± 0.5 $^{\circ}\text{C}$ using a regulated heating pad with a rectal probe (TR-200, FST, Foster City, CA, USA) and blood oxygen saturation was maintained using the anesthesia machine (RWD Life Science Co., Ltd., Shenzhen, China). A pulse oximeter clipped to the hind paw was used to monitor blood oxygen saturation and heart rate (MouseOx; Starr Life Sciences Corp., Oakmont, PA, USA). Systolic and diastolic blood pressure was recorded using a tail cuff pressure transducer (BP-98A; Softron Co. Ltd., Tokyo, Japan). To prevent low blood sugar or water loss during the surgery and imaging, the glucose was injected subcutaneously every 6 h during the surgery and imaging. The physiological parameters on fish oil-treated mice and *fat-1* mice during surgery and imaging were shown in Supplemental Tables 1 and 2, respectively. The animals with normal physiological parameters including body temperature, blood oxygen saturation, heart rate and mean arterial pressure were proceeded for further study and the animals with abnormal physiological parameters were excluded from the study. All animals were allowed to

recover for 24 h in a recovery cage post-surgery under a heat lamp and ad libitum access to drinking water and eating food.

2.9. Histologic Analysis

At 6 h, 1 d, 3 d, and 7 d after PAO and at 3 d, 7 d, and 14 d after induction of multiple diffuse microinfarcts, the animals were transcardially perfused with 50 ml ice-cold saline and fixed with 100 ml 4% paraformaldehyde (wt/vol). Brains were post-fixed overnight at 4 $^{\circ}\text{C}$ and then dehydrated by equilibration with 30% sucrose (wt/vol). For the animals with PAO, we removed the ipsilateral cortex within the frame of the thinned-skull window and placed it between two glass slides separated by a distance of 1.0 mm before post-fixation. For the animals with multiple diffuse microinfarcts, the brain tissues between the bregma and lambda were isolated. Brain sections, 10 μm thick, were then consecutively cut tangential to the cortical surface with a cryostat microtome (Leica Microsystems Inc., Jena, Germany). Selected sections were used for immunostaining, TUNEL staining, or Hematoxylin-eosin (HE) staining. For details, please refer to the Supplementary data.

2.10. TUNEL-Positive Cell Quantification

To quantify the number of TUNEL-positive cells after PAO, 8 brain sections from each animal, separated by 100 μm , were selected for TUNEL staining with a Fluorescein kit (Roche Applied Science, Penzberg, Germany) according to the manufacturer's instructions. The images were acquired with an Olympus fluorescence microscope (20 \times magnification). The number of TUNEL-positive cells was calculated using a computer-assisted mapping and cell quantification program (ImageJ software, NIH, Bethesda, MD, USA). The quantifications were performed by an investigator who was blind to the experiment.

2.11. Western-Blot Analysis

For protein analysis, mice in the fish oil group and control group were transcardially perfused with 50 ml ice-cold saline at 3 h, 24 h and 72 h after PAO ($n = 3$ at each time point per group). In addition, 4 mice with sham surgery were transcardially perfused with 50 ml ice-cold saline. The ipsilateral cortex within the frame of the thinned-skull window was then rapidly removed for protein isolation. The analysis was performed by an investigator who was blind to the experiment. For details, please refer to the Supplementary data.

2.12. Microinfarct Volume in PAO

To quantify the microinfarct volume at day 7 after PAO, we selected sections every other 9 sections and performed double immunostaining of NeuN and Iba1 on selected sections. The microinfarct border was identified as the boundary between the infarcted area devoid of NeuN-positive cells and occupied by clusters of activated microglia and the normal tissue exhibiting dense NeuN-positive cells. The microinfarct volume was calculated as described previously [40]. Briefly, serial images of the microinfarct were collected under an Olympus fluorescence microscope (20 \times magnification). The region of tissue damage in a series of adjacent brain sections was measured and the total infarct volume, V_t , was determined by $V_t = (V_1 + V_2 + \dots + V_n) d$, where V_n was the region of damage in the n th slice, and d was the distance between adjacent sections. The image collections and quantifications were performed by an investigator who was blind to the experiment.

2.13. Lesion Burden Analysis in Multiple Diffuse Microinfarcts

To quantify the lesion burden at 7 d and 14 d after the multiple diffuse ischemic injury, we outlined the lesion visualized by HE staining and then calculated the lesion area. The lesion burden was defined as the percentage of the total lesion area relative to the contralateral specific cerebral

region (cortex, hippocampus and subcortex). The average lesion burden per animal was determined by $(A1 + A2 + \dots + An)/n$, where An was the lesion burden in the n th slice, and n was the total number of brain slices used for lesion burden analysis. The quantifications were performed by an investigator who was blind to the experiment.

2.14. Behavioral Test

All the behavioral tests were performed by the researchers who were blind to the animal grouping. To evaluate whether multiple diffuse microinfarcts caused behavioral damage, animals underwent behavioral tests including open field exploration test, novel-object recognition, and Morris Water Maze test to investigate spontaneous anxiety, cognitive function, and hippocampal-based learning and short-term memory at 3 d, 7 d, and 14 d after surgery. For details, please refer to the Supplementary data.

2.15. Statistical Analysis

Statistical analyses of collected data were performed using data analysis software system SPSS 23.0. All values were expressed as the mean \pm SEM. Quantitative data distributions were tested for normality using Shapiro–Wilk's test. We performed power analysis on the sample size of each experiment using analysis software PASS 11.0. Differences in physiological parameters, the number of TUNEL-positive cells, protein expression associated with the RIPK1 and RIPK3 pathways, and behavioral performance among the sham surgery group, the control group, and the fish oil group were compared by one-way ANOVA followed with Dunnett's post hoc test. Differences in the PUFA composition, the volume of blood flux, the number of PI-positive cells, the microinfarct volume, and the lesion burden between the control group and the fish oil group or between the WT littermates and *Fat-1* mice were compared by unpaired student's *t*-tests. All the graphs were prepared using GraphPad Prism 5 (GraphPad Software Inc., La Jolla, CA, USA). Significance was defined as $P < 0.05$ in all the statistical analyses.

3. Results

3.1. Characterization of Ischemic Lesions Following PAO

We first imaged the mouse brain surface vasculature using two-photon laser-scanning microscopy (TPLSM) which revealed the surface communicating arteriole network and penetrating arterioles after labeling the blood plasma with FITC-d2000 (Fig. 1a and b). Penetrating arterioles were confirmed by the morphology and blood flow direction. The diameter of the penetrating arteriole was measured by high-resolution planar images and the red blood cell (RBC) velocity was measured by line-scans [37]. The blood flux of the penetrating arterioles of interest was calculated with the formula: $F = \pi/8 v (0) d^2$ [40]. A penetrating arteriole with a diameter from 15 to 25 μm and a centerline RBC velocity from 3.0 to 4.5 m/s was selected as the target vessel (Fig. 1b and c). Only one penetrating arteriole was selected as the target vessel per animal. After the target penetrating arteriole was selected, a clot was generated by Femtosecond Laser Ablation (Fig. 1c; Supplemental Video 1).

We employed the transcranial PI-staining to indicate the cell damage in vivo. We imaged the area supplied by the target penetrating arteriole from the cortical surface to below 300 μm at 0 min, 1 h, 3 h, 6 h, 12 h, 24 h, and 48 h after PAO using TPLSCM. The region of hypoperfusion appeared immediately in the core of the area supplied by the target penetrating arteriole and gradually expanded over time after the clot formation (Fig. 1d; $n = 3$). The PI-positive cells were initially observed in the hypoperfused area at 6 h after the clotting and their number increased gradually over time (Fig. 1d and e; $n = 3$), suggesting that there was a significant parenchymal cell loss after PAO. TUNEL-staining confirmed cell loss after PAO, as the apoptotic cells were clearly present

in the core of the ischemic lesion at 1 d, 3 d and 7 d after PAO (Fig. 1f and g; $n = 3$ per time point).

HE staining revealed that PAO led to a highly localized, nominally cylindrical region of tissue infarction (Supplemental Fig. 1a; $n = 3$). Immunostaining showed that the ischemic lesions were devoid of NeuN-positive neurons and filled with activated microglia and astrocytes (Supplemental Fig. 1b and 1c; $n = 3$). TUNEL-positive cells were found to be present in the cylindrical region of tissue infarction and many of them were surrounded by Iba1-positive microglial cells (Supplemental Fig. 1d and e). These Iba1-positive microglial cells co-expressed CD68, suggesting that they might be activated microglia with phagocytosing function (Supplemental Fig. 1f; $n = 3$).

3.2. ω -3 PUFAs Attenuated Ischemic Injury Induced by PAO

We next investigated whether ω -3 PUFAs could mitigate the cell loss after PAO. We fed C57BL/6 mice fish oil for 3 weeks prior to PAO and then analyzed the fatty acid profiles in the cortex by GC–MS. DHA, a major component of ω -3 PUFAs, was found to be significantly increased in the animals fed with fish oil compared with those without fish oil treatment (Supplemental Table 3; $n = 3$ per group). The baseline of the RBC speed and vessel diameter (pre-occlusion) of the target penetrating arteriole was measured and the baseline of blood flux was calculated before PAO. The baseline of blood flux in the target penetrating arteriole did not differ between the control group and the fish oil group (Fig. 2a and b; $n = 6$ per group). PI-positive cells in the ischemic lesion of fish oil-treated animals were found to be significantly lower than those in control animals at 24 h after PAO (Fig. 2a and c; $n = 6$ per group). Similarly, TUNEL staining demonstrated that the number of TUNEL-positive cells was markedly decreased in the fish oil-treated animals compared to the control at day 1 after PAO (Fig. 2d and e; $n = 6$ per group). We also measured the microinfarction volume at day 7 after PAO by histological analysis. The results revealed that ω -3 PUFAs substantially reduced the size of cerebral microinfarcts in fish oil-treated animals compared to the control animals (Fig. 2f and g; $n = 6$ per group).

To further confirm the protective effect of ω -3 PUFAs on attenuating the ischemic injury induced by PAO, the transgenic *Fat1* mouse that expresses the *Fat1* gene encoding a protein that converts ω -6 PUFAs to ω -3 PUFAs was used. The GC–MS analysis results demonstrated that the level of ω -3 PUFAs, such as DHA and docosapentaenoic acid (DPA), in the cortex of *Fat1* mice was significantly elevated compared with their WT littermates (Supplemental Table 4; $n = 3$ per group). The number of PI-positive cells and TUNEL-positive cells was significantly decreased in *Fat1* mice at day 1 after PAO compared with the WT counterparts (Supplemental Fig. 2a–e; $n = 6$ per group). In addition, the microinfarct volume was also found to be significantly reduced in *Fat1* mice compared with the WT counterparts at day 7 after PAO (Supplemental Fig. 2f–g; $n = 6$ per group). These results suggest that abundant endogenous ω -3 PUFAs also protect mice against PAO-induced ischemic injury.

3.3. ω -3 PUFAs Inhibited RIPK1-Mediated Apoptotic Pathway Following PAO

Necrosis and apoptosis are two main forms of neuronal cell death after focal ischemic stroke [50]. Cell death induced by various insults can be generally classified as either apoptosis or a form of necrosis which is correspondingly regulated by the receptor-interacting serine/threonine protein kinases 1 (RIPK1) and receptor-interacting serine/threonine protein kinases 3 (RIPK3) pathways, respectively [24]. To establish which pathway is responsible for neuronal loss after PAO, we determined the time-dependent alteration in protein expression associated with the RIPK1 and RIPK3 pathways at 3 h, 24 h and 72 h after PAO. The results revealed that the expression level of the apoptosis-related molecules, RIPK1, cleaved caspase 8 and cleaved caspase 3, were remarkably increased at 3 h after PAO and reached their peak at 24 h after PAO (Fig. 3a, b, e and f; $n = 3$ per group), whereas no obvious

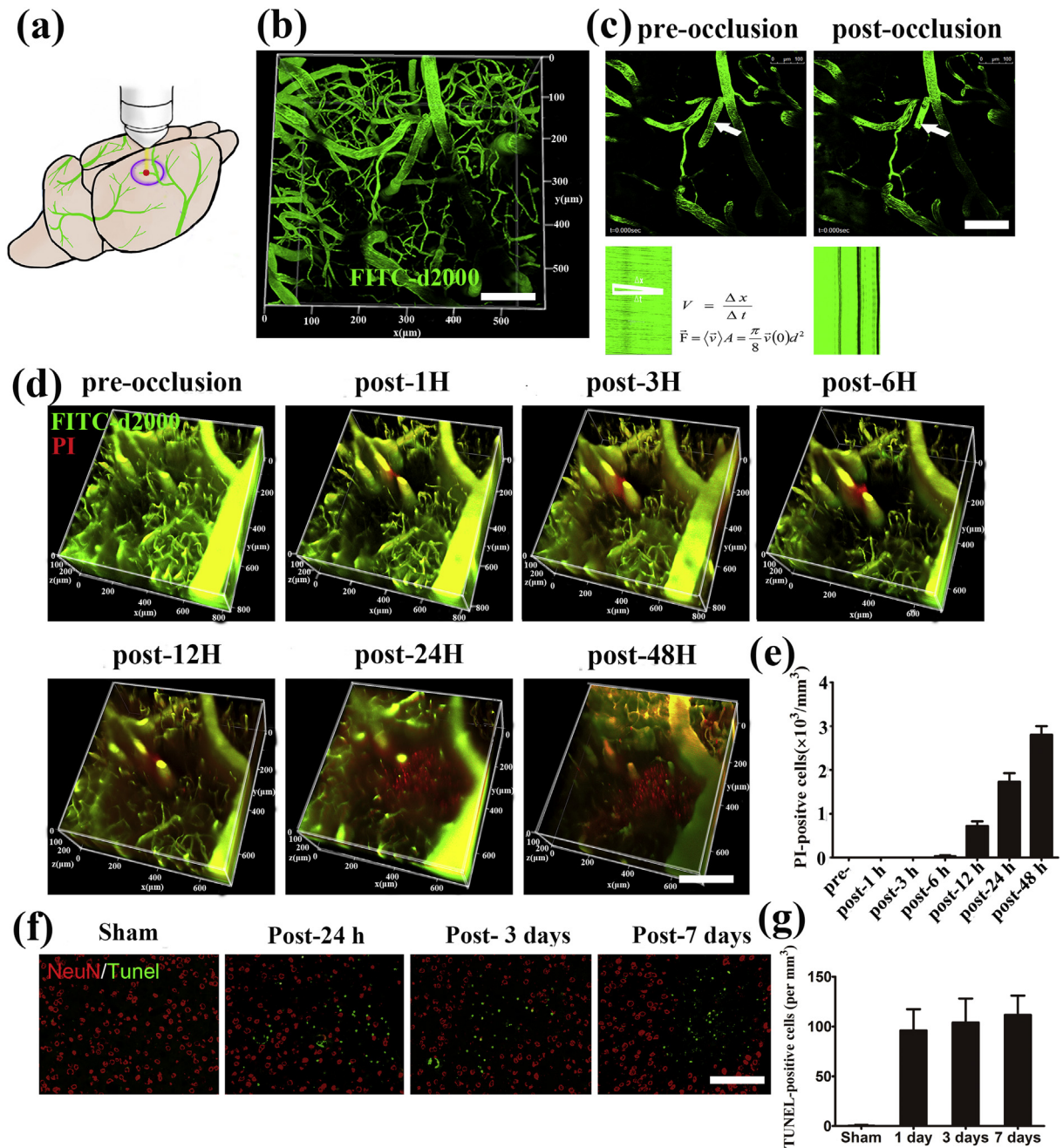


Fig. 1. Characterization of ischemic lesions after penetrating arteriole occlusion (PAO). (a) Schematic illustration of the occlusion of the target penetrating arteriole by two-photon microscopy. (b) A representative 3-D reconstructed image showing the cortical angioarchitecture in mice. (c) Two-photon image showing the change in the targeted arteriole (arrowed) and its red blood cell velocity before and after occlusion. (d) Representative images showing the dynamic evolution of microcirculation (labeled with FITC-d2000) and damaged cells (labeled with PI, red) at 0, 1, 3, 6, 12, 24 and 48 h after PAO. (e) Quantitative data showing that the number of PI-positive cells increased gradually over time after the occlusion (n = 3). (f) Representative images showing cell apoptosis (TUNEL staining, green) at days 1, 3, and 7 after PAO. (g) Quantitative analysis showing that the number of apoptotic cells were comparable at days 1, 3, and 7 after PAO (n = 3). Scale bar: 300 μm for a2, 250 μm for a3, 200 μm for b1 and 100 μm for b2.

alterations were found in the expression of the necrosis-related molecules RIPK3 and mixed lineage kinase domain-like (MLKL) at any time point after PAO (Fig. 3a, c and d; n = 3 per group). These findings indicate that PAO mainly activated the RIPK1-mediated apoptotic pathway, rather than the RIPK3-mediated necrosis pathway. We then determined the cell types undergoing apoptosis after PAO. Double immunostaining showed that cleaved caspase 8 and cleaved caspase 3, the two key apoptotic proteins, were co-expressed with the neuronal marker NeuN rather than with the microglial cell marker Iba1 and the astrocyte marker GFAP at 6 h after PAO (Supplemental Fig. 3; n = 3 per group), suggesting that PAO induced apoptosis mainly on neuronal cells.

Notably, administration of fish oil significantly inhibited PAO-induced activation of RIPK1 and its downstream apoptosis-associated proteins (Fig. 3a, b, e and f; n = 3 per group), which strongly indicates that ω -3 PUFAs attenuate the PAO-induced cell death in the cortex, possibly by inhibiting the RIPK1 mediated apoptotic pathway.

3.4. ω -3 PUFAs Confer Beneficial Effects in the Mouse Model with Multiple Diffuse Microinfarcts

A mouse model of multiple diffuse cerebral microinfarcts was established by unilateral injection of cholesterol crystals into the right

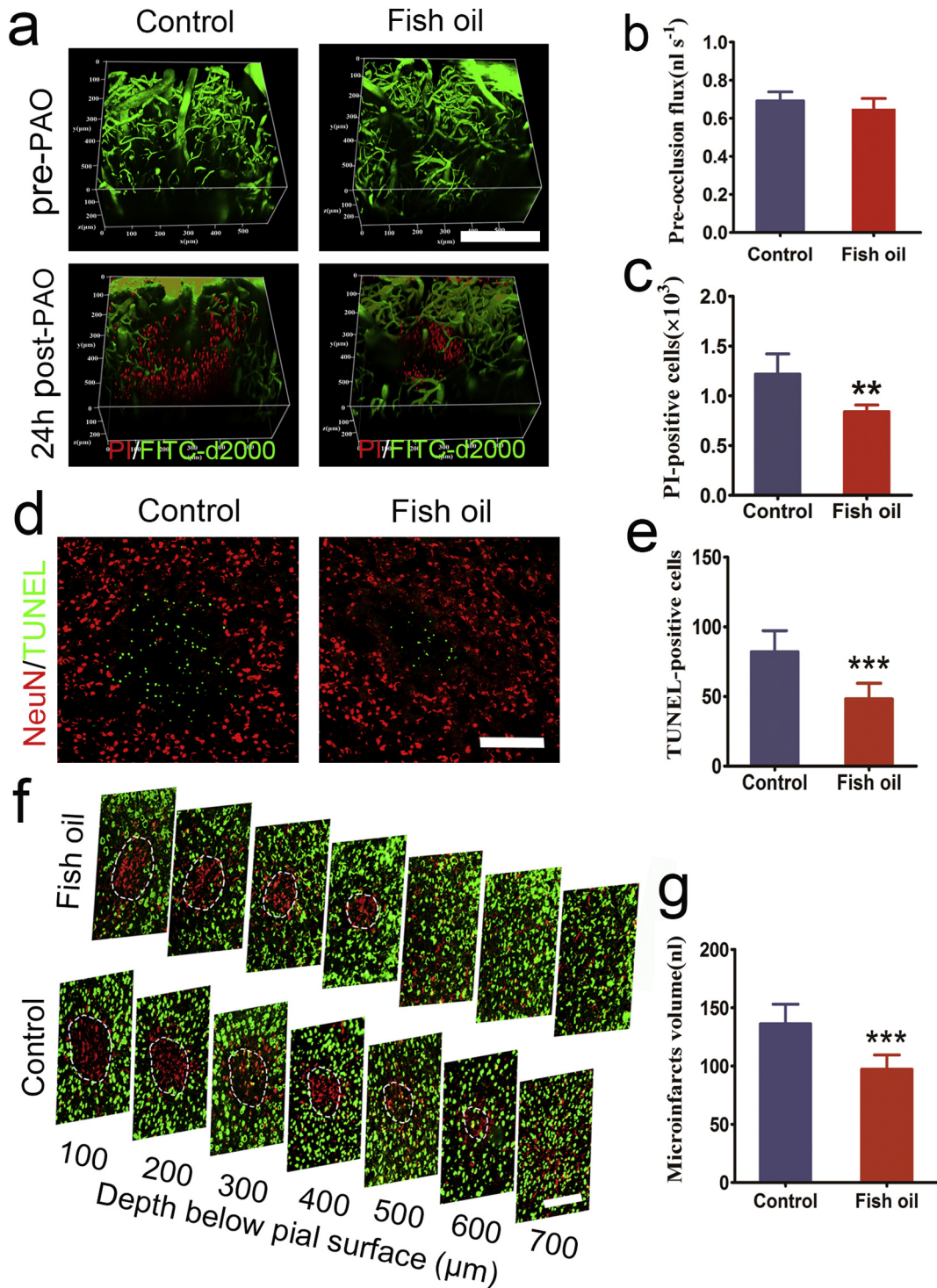


Fig. 2. Administration of fish oil attenuated ischemic injury induced by PAO. (a) Representative 3-D reconstructed images showing in vivo PI-labeling at 24 h after PAO in the control and fish oil groups. (b) Quantitative data revealed that the blood flux of the target vessel did not differ between the control group and fish oil group ($P > 0.05$, $n = 6$). (c) Quantitative analysis of PI-positive cells showed that the number of PI-positive cells in fish oil-treated animals was significantly lower than that in the control animals at 24 h after PAO (** $P < 0.01$, t -test, $n = 6$, power = 1.000). (d) Representative images showing TUNEL-positive staining (green) on coronal sections at 24 h after PAO in the control animals and fish oil-treated animals. (e) Quantitative analysis showing that the number of TUNEL-positive cells was markedly decreased in the fish oil-treated animals compared to the control group (** $P < 0.005$, t -test, $n = 6$, power = 0.99676). (f) Representative images of the infarcted tissue at d 7 after PAO, as delineated by NeuN staining (green) and Iba1 staining (red) over a depth of 700 μm below the pial surface. (g) Quantitative analysis of the microinfarct volume showing that administration of fish oil substantially reduced the size of cerebral microinfarcts compared to the control animals (** $P < 0.005$, t -test, $n = 6$, power = 0.98617). Scale bar: 300 μm for a, 200 μm for d, and 150 μm for f.

internal carotid artery (Fig. 4a). Using this model, we investigated the protective effect of ω -3 PUFAs on mitigating multiple diffuse microinfarcts. Microinfarcts were found throughout the right brain region such the cortex, subcortical tissue (consisting of striatum and

thalamus), and hippocampus as revealed by diffuse foci filled with Iba1 positive staining and devoid of NeuN staining (Fig. 4b). Compared with the control group, the number of TUNEL-positive cells in the cortex, hippocampus, and subcortical tissue of fish oil-treated animals

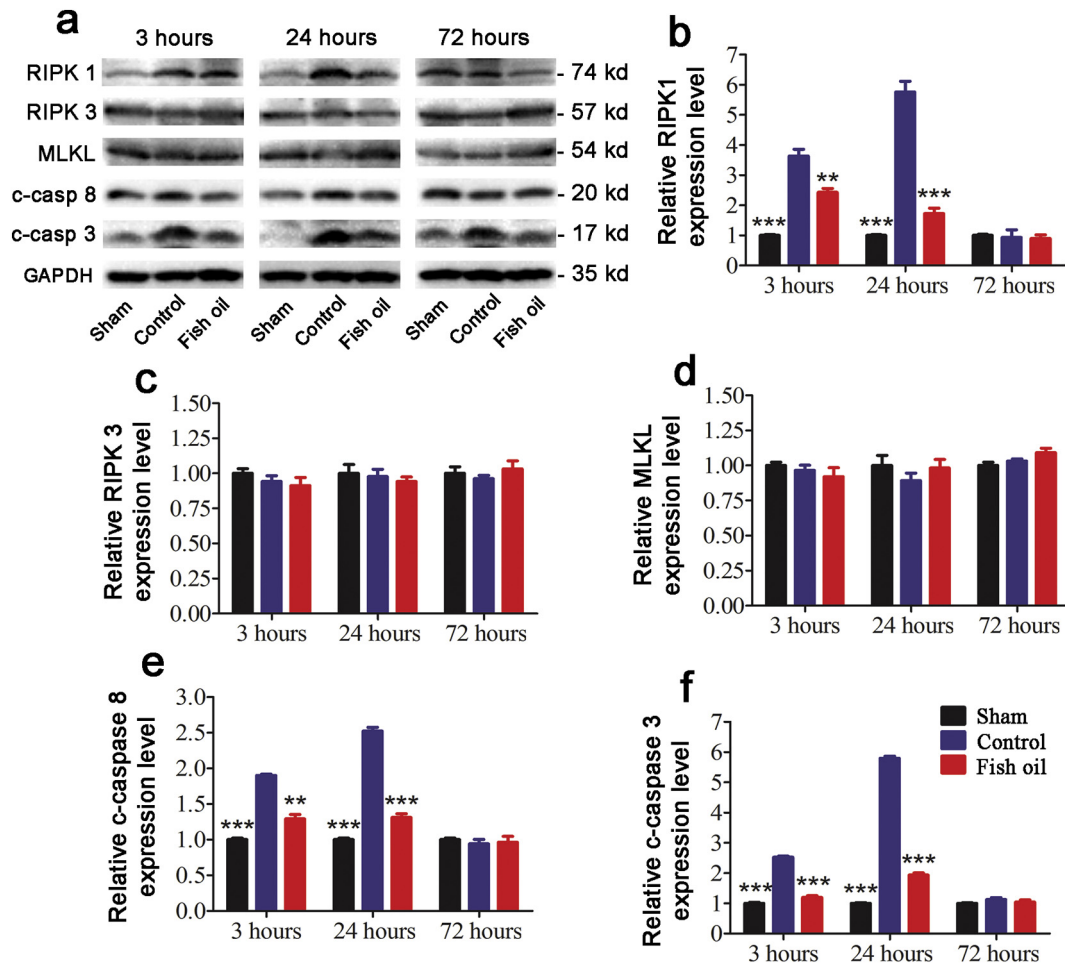


Fig. 3. Administration of fish oil inhibited the RIPK1-mediated apoptotic pathway after PAO. (a) Representative Western blots of apoptosis-related molecules (RIPK1, caspase 8 and caspase 3) and necrosis-related molecules (RIPK3 and MLKL) at 3, 24, and 72 h after PAO in the group of sham control, PAO, and PAO plus fish oil-treated. (b) Quantitative data of the relative expression of RIPK1. PAO significantly increased RIPK1 expression, whereas oil fish treatment markedly inhibited the PAO-induced RIPK1 activation (** $P < 0.01$; *** $P < 0.001$; one-way ANOVA; at 3 h after PAO, $n = 3$, power = 1.000; at 24 h after PAO, $n = 3$, power = 1.000). (c) Quantitative data of the relative expression of RIPK3. No difference in the expression of RIPK3 was found between before PAO and after PAO, and between the control group and oil fish group ($n = 3$). (d) Quantitative data of the relative expression of MLKL. No difference in the expression of MLKL was found between before PAO and after PAO, and between the control group and oil fish group ($n = 3$). (e) Quantitative data of the relative expression of caspase 8. PAO significantly increased caspase 8 expression, whereas oil fish treatment markedly inhibited the PAO-induced caspase 8 activation (** $P < 0.01$; *** $P < 0.001$; one-way ANOVA; at 3 h after PAO, $n = 3$, power = 0.996; at 24 h after PAO, $n = 3$, power = 0.999). (f) Quantitative data of the relative expression of caspase 3. PAO significantly increased caspase 3 expression, whereas oil fish treatment markedly inhibited the PAO-induced caspase 3 activation (** $P < 0.01$; *** $P < 0.001$; one-way ANOVA; at 3 h after PAO, $n = 3$, power = 0.999; at 24 h after PAO, $n = 3$, power = 1.000).

was markedly decreased at 3 d after the surgery (Fig. 4c; $n = 4$ per group).

Consistent with these results, HE staining showed that the lesion burden in the cortex, hippocampus and subcortical tissue was markedly attenuated at 7 d and 14 d after introduction of multiple diffuse microinfarcts in fish oil-treated animals compared to the control animals (Fig. 5; $n = 4$ per group at each time point).

The induction of multiple diffuse cerebral microinfarcts leads to cognitive deficits in mice [47]. In this study, at 3 d and 7 d after induction of multiple diffuse cerebral microinfarcts, the injured animals exhibited significantly reduced time spent in the center as evidenced by the open field test as compared to the sham surgery group (Fig. 6a; $n = 6$ per group at each time point), indicating that diffuse cerebral microinfarcts increased spontaneous anxiety. The injured animals also showed markedly reduced preference for the novel object as compared to the sham surgery group (Fig. 6b; $n = 6$ per group at each time point), indicating a decline in cognitive function. The fish oil-treated animals exhibited a significant reduction of anxiety expression evidenced by the open field exploration test and a significant increase in preference for the novel object evidenced by the novel object recognition test at 3 d and 7 d compared to the control animals (Fig. 6a and b; $n = 6$ per group at each time point). At 14 d, both the open field test and the novel object recognition test showed that

spontaneous anxiety and novel object recognition returned to the normal level in the animals with multiple diffuse cerebral microinfarcts (Fig. 6a and b; $n = 6$ per group at each time point), suggesting that there is an automatic recovery in spontaneous anxiety and novel object recognition in mice with multiple diffuse cerebral microinfarcts. The results of the Morris Water Maze test demonstrated that the animals with multiple diffuse cerebral microinfarcts exhibited deficient hippocampal-based learning and short-term memory at 3 d, 7 d, and 14 d as indicated by the significantly increased time finding the hidden platform and the reduced number of crossings in the target area in the probe trial (Fig. 6c and d; $n = 6$ per group at each time point). In accordance with the reduction of cell loss and lesion burden after fish oil treatment, the hippocampal-based learning and short-term memory were significantly improved in fish oil-treated animals at 3 d, 7 d, and 14 d compared with the control animals as indicated by Morris Water Maze test (Fig. 6c and d; $n = 6$ per group at each time point).

4. Discussion

This study, to the best of our knowledge, is the first to demonstrate that ω -3 PUFAs have protective effects against microinfarcts by inhibiting apoptosis, mitigating tissue damage, and thus improving

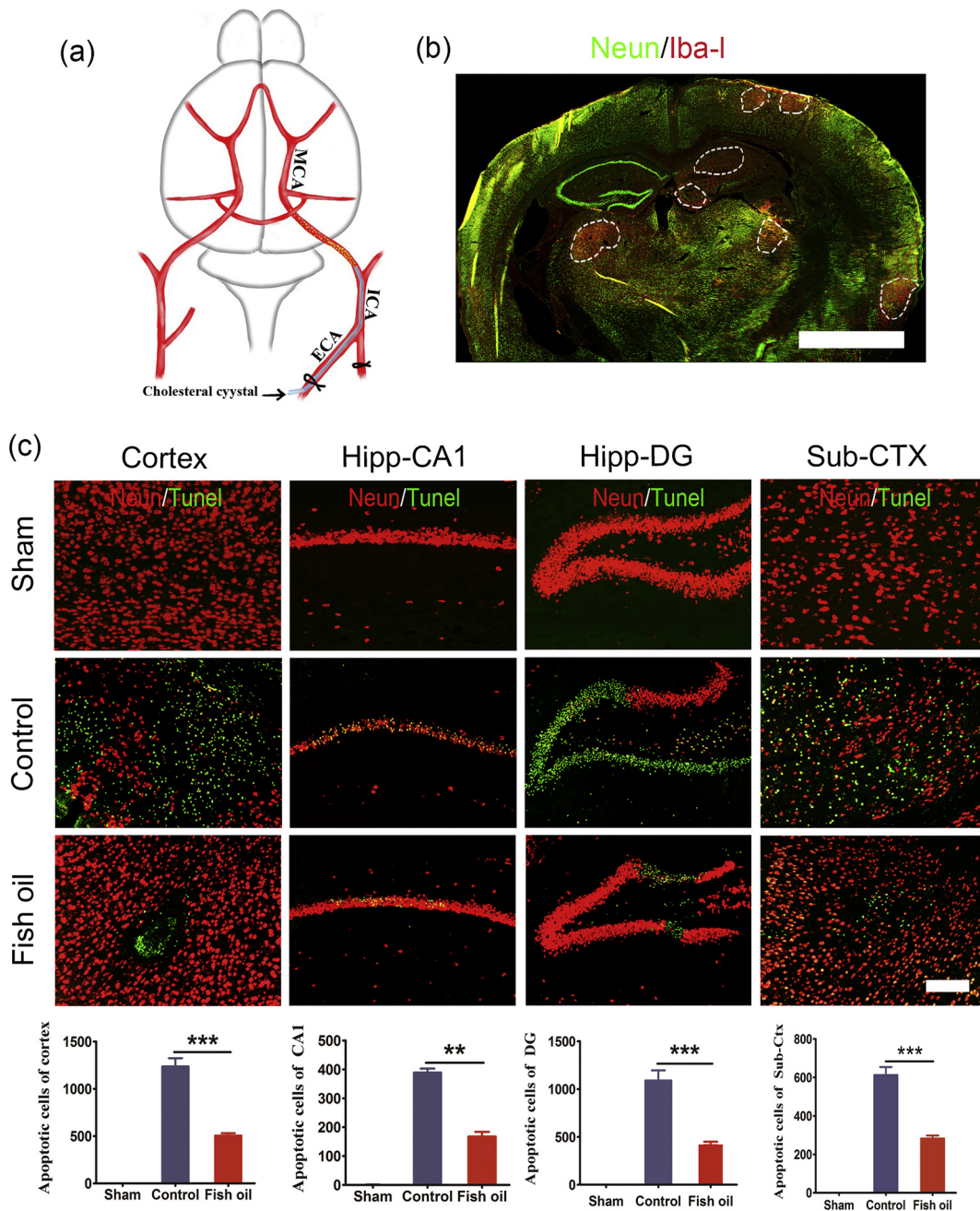


Fig. 4. Administration of fish oil protected mice against multiple diffuse microinfarcts. (a) Schematic illustration of a multiple diffuse microinfarcts model. (b) A representative image at low magnification depicting the microinfarct burden in the various brain regions as revealed by the diffuse foci with activated microglia (Iba1-positive; red) and absence of neurons (NeuN-positive; green) in the core. (c) Apoptosis in different brain regions of the control and fish oil-treated animals (NeuN staining for neuron, red; TUNEL staining for apoptotic cells, green). Compared with the control group, fish oil treatment significantly attenuated apoptosis in the various brain regions, such as the cortex, hippocampus and sub-cortex (Consisting of striatum and thalamus) (** $P < 0.01$; *** $P < 0.001$; cortex: one-way ANOVA, $n = 4$, power = 0.999; CA1: one-way ANOVA, $n = 4$, power = 1.000; DG: one-way ANOVA, $n = 4$, power = 0.996; Sub-cortex: one-way ANOVA, $n = 4$, power = 1.000). Scale bar: 2 mm for b, and 150 μm for c.

cognitive impairment. Microinfarcts are very common in aging brains and considered to be an independent risk factor of common neuropsychiatric disorders. Since the pathological mechanisms underlying the evolution of microinfarcts are not yet fully understood, therapeutic interventions against these microvascular ischemic lesions are still inadequate. This study provides a nutraceutical approach which can be potentially applied to clinical treatment and prevention of vascular dementia in the geriatric population.

The main findings of our study is that exogenously-delivered and endogenously-generated ω -3 PUFAs contribute to anatomically decreasing microinfarct damage, as revealed by the reduction of the

volume of microinfarct areas and number of PI-positive and TUNEL-positive cells (Fig. 2; Supplementary Fig. 2). The PAO-induced microinfarct model using femtosecond laser ablation by TPLSCM is considered a useful animal model to investigate the pathophysiological events leading to the formation of microinfarction. Using TPLSCM, the pathophysiological events, such as microcirculation alteration and cell death, could be directly monitored in vivo. Our previous study demonstrated that occluding penetrating arterioles immediately led to significant hypoperfused damage in the core area supplied by the target penetrating arterioles [21]. Consistent with the evolution of hypoperfusion, we detected cell death in the core region of hypoperfusion at 6 h in most animals,

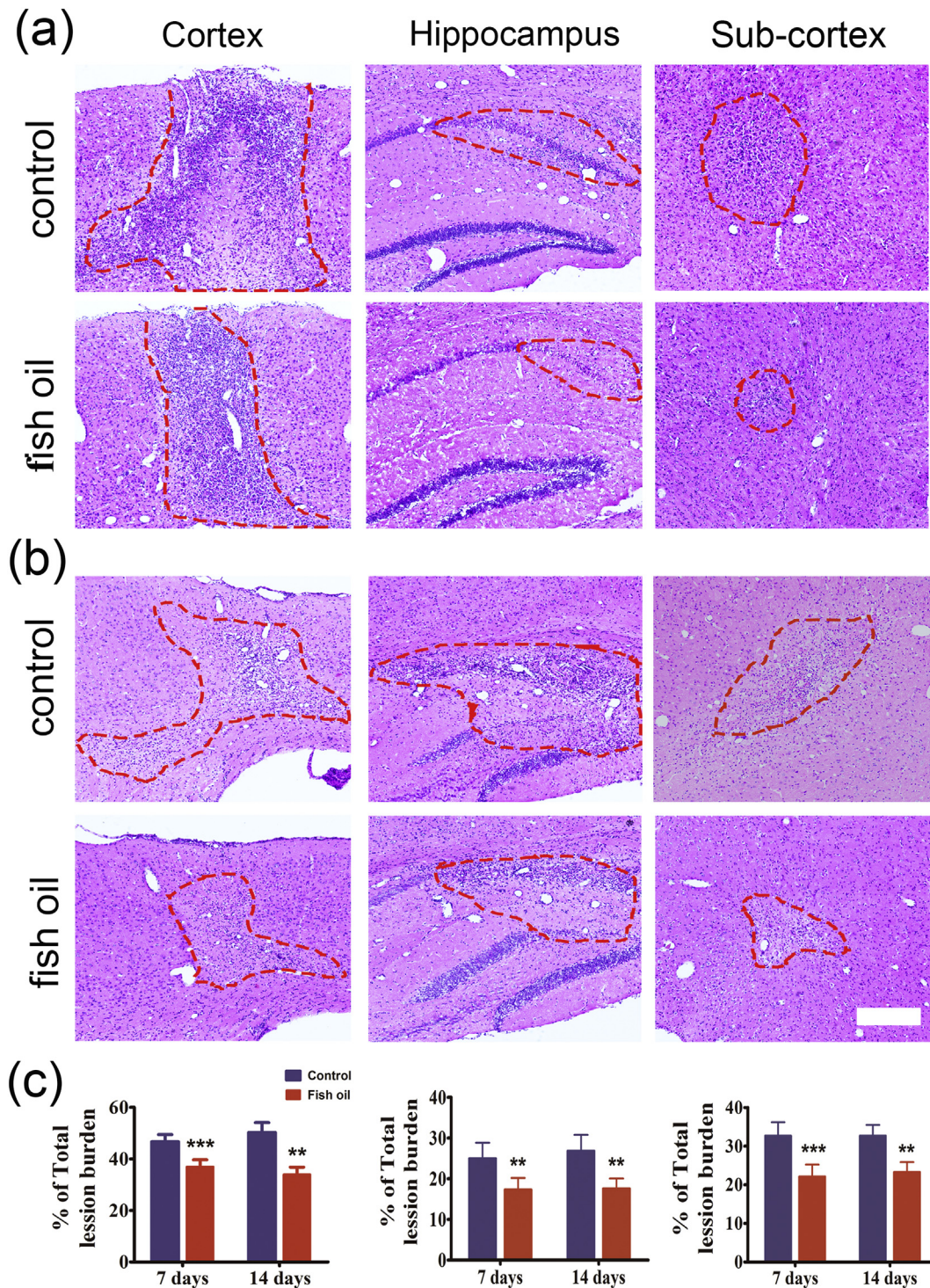


Fig. 5. Administration of fish oil alleviated the lesion burden in the specific cerebral region in a mouse model of multiple diffuse microinfarcts. a. HE staining showing the lesion in the cortex, hippocampus and sub-cortex at 7 d after the surgery (the red dotted line represents the lesion zone). b. HE staining showing the lesion in the cortex, hippocampus and sub-cortex at 14 d after the surgery (the red dotted line represents the lesion zone). c. Compared with the control group, fish oil treatment significantly attenuated the lesion burden in the cortex, hippocampus and sub-cortex (Consisting of striatum and thalamus) (** $P < 0.01$; *** $P < 0.001$; cortex: t -test, at 7 days after the surgery, $n = 4$, power = 0.895; at 14 days after the surgery, $n = 4$, power = 0.932; hippocampus: t -test; at 7 days after the surgery, $n = 4$, power = 0.884; at 14 days after the surgery, $n = 4$, power = 0.933; sub-cortex: t -test; at 7 days after the surgery, $n = 4$, power = 0.888; at 14 days after the surgery, $n = 4$, power = 0.916). Scale bar: 200 μm .

which increased gradually over time until 48 h after the formation of the clot. Pathological analysis has shown that microinfarcts induced by PAO are mostly partial because the core of the ischemic lesion was filled with apoptotic cells and activated microglia and astrocytes, which is significantly different from the traditional focal ischemic lesions. To extend our previous findings, we applied two microvascular ischemic models

and successfully demonstrated the beneficial effects of ω -3 PUFAs against microinfarcts in both the *Fat1* mice with endogenously-enriched ω -3 PUFAs and the mice with exogenously-delivered fish oil diets.

It has been reported that within the first 24 h after middle cerebral artery occlusion (MCAO), a typical traditional focal ischemic model,

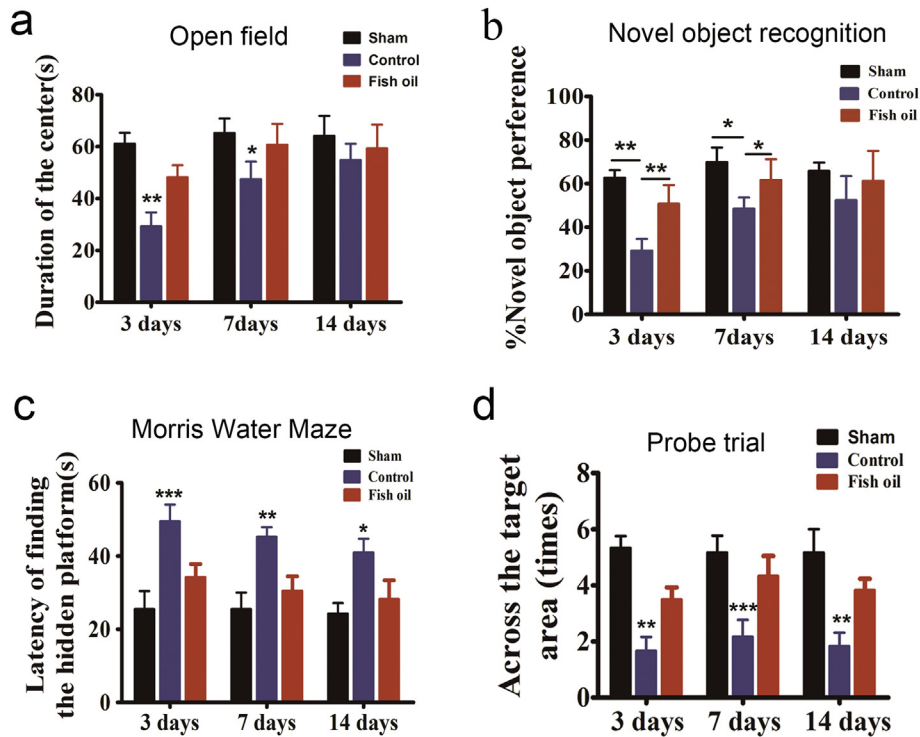


Fig. 6. Administration of fish oil significantly improved the anxiety-like behavior, cognitive function, and hippocampal-based learning and short-term memory in a mouse model of multiple diffuse microinfarcts. (a) The open field test (* $P < 0.05$; ** $P < 0.01$; *** $P < 0.001$; one-way ANOVA; at 3 days after surgery, $n = 6$, power = 0.984; at 7 days after PAO, $n = 6$, power = 0.976). (b) The novel object recognition (* $P < 0.05$; ** $P < 0.01$; *** $P < 0.001$; one-way ANOVA; at 3 days after surgery, $n = 6$, power = 1.000; at 7 days after PAO, $n = 6$, power = 1.000). (c) The memory retention test (* $P < 0.05$; ** $P < 0.01$; *** $P < 0.001$; one-way ANOVA; at 3 days after surgery, $n = 6$, power = 1.000; at 7 days after PAO, $n = 6$, power = 1.000; at 14 days after surgery, $n = 6$, power = 0.917). (d) The space probe trial. (* $P < 0.05$; ** $P < 0.01$; *** $P < 0.001$; one-way ANOVA; at 3 days after surgery, $n = 6$, power = 0.991; at 7 days after PAO, $n = 6$, power = 0.998; at 14 days after surgery, $n = 6$, power = 0.985).

the core of ischemic lesion presents necrosis, and the penumbra surrounding the core presents apoptosis [7,16,18]. However, cerebral microinfarcts are mostly incomplete and appear as neural cell loss with gliosis, suggesting that there are distinct pathophysiological events between microinfarcts and traditional focal ischemic lesions. An additional main finding of this study is that ω -3 PUFAs can inhibit the RIPK1-mediated apoptotic pathways involved in the neuronal cell loss and activation of glial cells observed in the ischemic core of cortical microinfarcts. Necrosis and apoptosis are two major forms of neuronal cell death after focal ischemic stroke [7]. Cell death induced by various insults can be generally classified as either apoptosis or a form of necrosis, which are regulated by the RIPK1-mediated and RIPK3-mediated pathway, respectively [48]. The kinase activity of RIPK1 has been implicated in apoptosis by activating caspase-8 to initiate the apoptotic demise of the cell [48]. Activation of RIPK3 and its interaction with pseudokinase substrate MLKL lead to cell death by necroptosis rather than apoptosis [43]. These two forms of neuronal cell death might be concomitantly activated in the same ischemic lesion and vary in a progressive manner [5]. The involvement of necrosis or apoptosis may depend on the severity of the ischemic injury, as well as the presence of reperfusion [46]. In the current study, we demonstrated that the PAO-induced ischemic injury activated the RIPK1-mediated apoptosis pathway rather than RIPK3-mediated necrosis pathway (Fig. 3), which supports the notion that apoptosis may play an important role in the evolution of microinfarcts in our model. More importantly, we also demonstrated that ω -3 PUFAs specifically decreased RIPK1, but not RIPK3 expression level in the PAO models.

The protective effects of ω -3 PUFAs against microinfarcts were further verified in a multiple diffuse microinfarcts model. Our study found that ω -3 PUFAs supplements significantly improved the functional deficits, which is in accordance with the reduction of cell loss and lesion burden. It should be noted that the sample size used for

behavioral analysis in our study (6 animals at each time point in each group) is relatively small. Behavioral studies in rodents are associated with significant variability. It should also be noted that the equation used to calculate the infarct volume in the study did not control for edema and the results obtained by the equation may overestimate the lesion volume because microinfarctions could lead to BBB damage, which causes edema due to water influx from plasma.

Accumulating evidence, including our previous studies, has shown that ω -3 PUFAs exhibit neuroprotective effects by suppressing nuclear factor-kappa B activation, inhibiting reactive oxygen species (ROS) production, heme oxygenase 1 activity and attenuating apoptosis [17,19,20,52]. In addition, cerebral vascular factors have been shown to have direct contributions to several neurobehavioral disorders [3,6,51]. The findings of this study are greatly strengthened by the anatomical observations after applying advanced TPLSM, as well as by the assessment of the effects of ω -3 PUFAs in both endogenously-enriched and exogenously-delivered animal models. These results suggest that supplement of ω -3 PUFAs is an effective pharmacological intervention for improving cognitive impairment in a mouse model with microvascular ischemic lesions via alleviating the burden of microinfarcts. However, it should be noted that although most epidemiological studies have reported that ω -3 PUFAs supplements confer benefits to human health, a growing body of literature has shown inconsistent data on the efficacy in ω -3 PUFAs supplements. A recent murine study demonstrated that there were no effects of fish oil supplementation on slowing aging or promoting longevity [22]. A meta-analysis including 20 randomized controlled trials with a total of 68,680 patients reported that ω -3 PUFAs supplements had no significant impact on lowering cardiovascular risk [23]. A large clinical trial with 4000 patients included showed that ω -3 PUFAs supplements did not slow cognitive decline in older people [8]. These reports suggest that more future work targeted on specific diseases and health problems with enough long duration is

needed to obtain consensus on the therapeutic potentials of ω -3 PUFAs supplements.

In summary, the present study demonstrates that ω -3 PUFAs could protect mice against microinfarcts and improve functional deficits by reducing the microinfarct burden. The study also provides evidence that targeting microinfarcts could be an effective strategy for ameliorating cognitive and behavioral impairment, and support the conduction of future clinical trials of ω -3 PUFAs in the treatment or prophylaxis in vascular dementia and depression.

Supplementary data to this article can be found online at <https://doi.org/10.1016/j.ebiom.2018.05.028>.

Acknowledgments

This study was supported by Macao Science and Technology Development Fund (020/2017/A1) and multi-year research grant, University of Macau, MYRG2016-00184-ICMS-QRCM, Natural Science Foundation of Guangdong Province (2016A030313675), and the National Key Clinical Department, National Key Discipline, and Guangdong Key Laboratory for diagnosis and treatment of major neurological disease. The authors thank Dr. Meng Wang for fatty acid analysis using GC–MS, and Mr. Qiang Liu for measurement of the volume of blood influx and image acquisition and analysis with PI staining.

Conflict of Interest

The authors declared no conflicts of interest.

Author Contributions

HS and CL designed the study; CL, HR, XY, ZS, FL performed the experiments; JK, JW, ZP, KS, and HS analyzed the results together; CL, KS and HS wrote the paper; all authors read and approved the final version.

References

- Alexopoulos GS. The vascular depression hypothesis: 10 years later. *Biol Psychiatry* 2006;60:1304–5.
- Amminger GP, McGorry PD. Update on ω -3 polyunsaturated fatty acids in early-stage psychotic disorders. *Neuropsychopharmacology* 2012;37:309–10.
- Arvanitakis Z, Leurgans SE, Barnes LL, Bennett DA, Schneider JA. Microinfarct pathology, dementia, and cognitive systems. *Stroke* 2011;42:722–7.
- Belayev L, Khoutorova L, Atkins KD, Eady TN, Hong S, Lu Y, et al. Docosahexaenoic acid therapy of experimental ischemic stroke. *Transl Stroke Res* 2011;2:33–41.
- Benchoua A, Guegan C, Couriaud C, Hosseini H, Sampaio N, Morin D, et al. Specific caspase pathways are activated in the two stages of cerebral infarction. *J Neurosci* 2001;21:7127–34.
- Blondeau N, Nguemni C, Debruyne DN, Piens M, Wu X, Pan H, et al. Subchronic alpha-linolenic acid treatment enhances brain plasticity and exerts an antidepressant effect: a versatile potential therapy for stroke. *Neuropsychopharmacology* 2009;34:2548–59.
- Broughton BR, Reutens DC, Sobey CG. Apoptotic mechanisms after cerebral ischemia. *Stroke* 2009;40:e331–e339.
- Chew EY, Clemons TE, Agrón E, Launer LJ, Grodstein F, Bernstein PS, et al. Effect of Omega-3 fatty acids, lutein/zeaxanthin, or other nutrient supplementation on cognitive function: the AREDS2 randomized clinical trial. *JAMA* 2015;314:791–801.
- De Reuck J, Deramecourt V, Auger F, Durieux N, Cordonnier C, Devos D, et al. Post-mortem 7.0-tesla magnetic resonance study of cortical microinfarcts in neurodegenerative diseases and vascular dementia with neuropathological correlates. *J Neurosci* 2014;34:85–9.
- Iadecola C. The pathobiology of vascular dementia. *Neuron* 2013;80:844–66.
- Kang JX, Wang J, Wu L, Kang ZB. Transgenic mice: fat-1 mice convert n-6 to n-3 fatty acids. *Nature* 2004;42:504.
- Kroger E, Laforce R. Fish consumption, brain mercury, and neuropathology in patients with Alzheimer disease and dementia. *JAMA* 2016;315:465–6.
- Lalancette-Hebert M, Julien C, Cordeau P, Bohacek I, Weng YC, Calon F, et al. Accumulation of dietary docosahexaenoic acid in the brain attenuates acute immune response and development of postischemic neuronal damage. *Stroke* 2011;42:2903–9.
- Launer LJ, Hughes TM, White LR. Microinfarcts, brain atrophy, and cognitive function: the Honolulu Asia aging study autopsy study. *Ann Neuro* 2011;70:774–80.
- Lee MJ, Seo SW, Na DL, Kim C, Park JH, Kim GH, et al. Synergistic effects of ischemia and β -amyloid burden on cognitive decline in patients with subcortical vascular mild cognitive impairment. *JAMA Psychiat* 2014;71:412–22.
- Linkermann A, Brasen JH, Darding M, Jin MK, Sanz AB, Heller JO, et al. Two independent pathways of regulated necrosis mediate ischemia-reperfusion injury. *Proc Natl Acad Sci U S A* 2013;110:12024–9.
- Liu Q, Wu D, Ni N, Ren H, Luo C, He C, et al. Omega-3 polyunsaturated fatty acids protect neural progenitor cells against oxidative injury. *Mar Drugs* 2014;12:2341–56.
- Love S. Apoptosis and brain ischaemia. *Prog Neuropsychopharmacol Biol Psychiatry* 2003;27:267–82.
- Lu DY, Tsao YY, Leung YM, Su KP. Docosahexaenoic acid suppresses neuroinflammatory responses and induces heme oxygenase-1 expression in BV-2 microglia: implications of antidepressant effects for ω -3 fatty acids. *Neuropsychopharmacology* 2010;35:2238–48.
- Luo C, Ren H, Wan JB, Yao X, Zhang X, He C, et al. Enriched endogenous omega-3 fatty acids in mice protect against global ischemia injury. *J Lipid Res* 2014;55:1288–97.
- Luo C, Liang F, Ren H, Yao X, Liu Q, Li M, et al. Collateral blood flow in different cerebrovascular hierarchy provides endogenous protection in cerebral ischemia. *Brain Pathol* 2017;27:809–21.
- de Magalhães JP, Müller M, Rainger GE, Steegenga W. Fish oil supplements, longevity and aging. *Aging (Albany NY)* 2016;8:1578–82.
- Monaco J, Mounsey A, Bello KJ. PURLs: should you still recommend omega-3 supplements? *J Fam Pract* 2013;62:422–4.
- Newton K. Ripk1 and ripk3: critical regulators of inflammation and cell death. *Trends in Cell Biol* 2015;25:347–53.
- Nishimura N, Schaffer C, Friedman B, Tsai PS, Lyden PD, Kleinfeld D. Targeted insult to subsurface cortical blood vessels using ultrashort laser pulses: three models of stroke. *Nat Methods* 2006;3:99–108.
- Nishimura N, Rosidi N, Iadecola C, Schaffer CB. Limitations of collateral flow after occlusion of a single cortical penetrating arteriole. *J Cereb Blood Flow Metab* 2010;30:1914–27.
- O'Brien JT, Thomas A. Vascular dementia. *Lancet* 2015;386:1698–706.
- Ortner M, Kurz A, Alexopoulos P, Auer F, Diehl-Schmid J, Drzezga A, et al. Small vessel disease, but neither amyloid load nor metabolic deficit, is dependent on age at onset in Alzheimer's disease. *Biol Psychiatry* 2015;77:704–10.
- Paranthaman R, Greenstein AS, Burns AS, Cruickshank JK, Heagerty AM, Jackson A, et al. Vascular function in older adults with depressive disorder. *Biol Psychiatry* 2010;68:133–9.
- Rao JS, Ertley RN, Lee HJ, DeMar Jr JC, Arnold JT, Rapoport SI, et al. N-3 polyunsaturated fatty acid deprivation in rats decreases frontal cortex BDNF via a p38 mapk-dependent mechanism. *Mol Psychiatry* 2007;12:36–46.
- Ren H, Yang Z, Luo C, Zeng H, Li P, Kang JX, et al. Enriched endogenous omega-3 fatty acids in mice ameliorate parenchymal cell death after traumatic brain injury. *Mol Neurobiol* 2017;54:3317–26.
- Roman GC, Erkinjuntti T, Wallin A, Pantoni L, Chui HC. Subcortical ischaemic vascular dementia. *Lancet Neurol* 2002;1:426–36.
- van Rooden S, Goos JD, van Opstal AM, Versluis MJ, Webb AG, Blauw GJ, et al. Increased number of microinfarcts in alzheimer disease at 7-t mr imaging. *Radiology* 2014;270:205–11.
- Roth TL, Nayak D, Atanasijevic T, Koretsky AP, Latour LL, McGavern DB. Transcranial amelioration of inflammation and cell death following brain injury. *Nature* 2014;505:223–8.
- Ruxton C, Reed S, Simpson M, Millington K. The health benefits of omega-3 polyunsaturated fatty acids: a review of the evidence. *J Hum Nutr Diet* 2007;20:275–85.
- Santos M, Gold G, Kovari E, Herrmann FR, Bozikas VP, Bouras C, et al. Differential impact of lacunes and microvascular lesions on poststroke depression. *Stroke* 2009;40:3557–62.
- Schaffer CB, Friedman B, Nishimura N, Schroeder LF, Tsai PS, Ebner FF, et al. Two-photon imaging of cortical surface microvessels reveals a robust redistribution in blood flow after vascular occlusion. *PLoS Biol* 2006;4:e22.
- Schoknecht K, Prager O, Vazana U, Kaminsky L, Harhausen D, Zille M, et al. Monitoring stroke progression: in vivo imaging of cortical perfusion, blood brain barrier permeability and cellular damage in the rat photothrombosis model. *J Cereb Blood Flow Metab* 2014;34:1791–801.
- Shi Z, Ren H, Luo C, Yao X, Li P, He C, et al. Enriched endogenous omega-3 polyunsaturated fatty acids protect cortical neurons from experimental ischemic injury. *Mol Neurobiol* 2016;53:6482–8.
- Shih AY, Blinder P, Tsai PS, Friedman B, Stanley G, Lyden PD, et al. The smallest stroke: occlusion of one penetrating vessel leads to infarction and a cognitive deficit. *Nat Neurosci* 2013;16:55–63.
- Simopoulos AP. Omega-3 fatty acids in health and disease. *Am J Clin Nutr* 1991;54:438–63.
- Smith EE, Schneider JA, Wardlaw JM, Greenberg SM. Cerebral microinfarcts: the invisible lesions. *Lancet Neurol* 2012;11:272–82.
- Sun L, Wang H, Wang Z, He S, Chen S, Liao D, et al. Mixed lineage kinase domain-like protein mediates necrosis signaling downstream of rip3 kinase. *Cell* 2012;148:213–27.
- Tosto G, Zimmerman ME, Carmichael OT, Brickman AM. Predicting aggressive decline in mild cognitive impairment: the importance of white matter hyperintensities. *JAMA Neurol* 2014;71:872–7.
- Tsopoulos C, Stewart R, Savva GM, Brayne C, Ince P, Thomas A, et al. Neuropathological correlates of late-life depression in older people. *Br J Psychiatry* 2011;198:109–14.
- Unal-Cevik I, Kilinc M, Can A, Gursoy-Ozdemir Y, Dalkara T. Apoptotic and necrotic death mechanisms are concomitantly activated in the same cell after cerebral ischemia. *Stroke* 2004;35:2189–94.
- Wang M, Iliff JJ, Liao Y, Chen MJ, Shinseki MS, Venkataraman A, et al. Cognitive deficits and delayed neuronal loss in a mouse model of multiple microinfarcts. *J Neurosci* 2012;32:17948–60.

- [48] Weng D, Marty-Roix R, Ganesan S, Proulx MK, Vladimer GI, Kaiser WJ, et al. Caspase-8 and rip kinases regulate bacteria-induced innate immune responses and cell death. *Proc Natl Acad Sci U S A* 2014;111:7391–6.
- [49] Yassine HN, Braskie MN, Mack WJ, Castor KJ, Fonteh AN, Schneider LS, et al. Association of docosahexaenoic acid supplementation with alzheimer disease stage in apolipoprotein E epsilon4 carriers: a review. *JAMA Neurol* 2017;74:339–47.
- [50] Yuan J. Neuroprotective strategies targeting apoptotic and necrotic cell death for stroke. *Apoptosis* 2009;14:469–77.
- [51] Yutsudo N, Kamada T, Kajitani K, Nomaru H, Katogi A, Ohnishi YH, et al. fosB-null mice display impaired adult hippocampal neurogenesis and spontaneous epilepsy with depressive behavior. *Neuropsychopharmacology* 2013;38:895–906.
- [52] Zhang M, Wang S, Mao L, Leak RK, Shi Y, Zhang W, et al. Omega-3 fatty acids protect the brain against ischemic injury by activating nrf2 and upregulating heme oxygenase 1. *J Neurosci* 2014;34:1903–15.